

Two-Electron Bound States in a Continuum in Quantum Dots[¶]

A. F. Sadreev^a and T. V. Babushkina^b

^a *Institute of Physics, Russian Academy of Sciences, Krasnoyarsk, 660036 Russia*

^b *Siberian Federal University, Krasnoyarsk, 660079 Russia*

Received May 4, 2008; in final form, July 16, 2008

A bound state in a continuum (BIC) might appear in open quantum dots for the variation in the dot's shape. By means of the equations of motion of the Green's functions, we investigate the effect of strong intradot Coulomb interactions on that phenomenon within the framework of the impurity Anderson model. The equation that the imaginary part of the poles of the Green's function equals zero yields the condition for BICs. As a result, we show that the Coulomb interactions replicate the single-electron BICs into two-electron ones.

PACS numbers: 05.60.Gg, 71.27.+a, 72.10.-d, 73.23.Hk

DOI: 10.1134/S0021364008170050

In 1929, von Neumann and Wigner [1] predicted the existence of discrete solutions of the single-particle Schrödinger equation embedded in the continuum of positive energy states. Their analysis, examined by Stillinger and Herrick [2], was regarded as a mathematical curiosity for a long time because of certain spatially oscillating central symmetric potentials. More recently in 1973, Herrik [3] and Stillinger [4] predicted BICs in semiconductor heterostructure superlattices which were observed by Capasso et al. [5] as the very narrow absorption peak.

Within the framework of Feshbach's theory of resonances, Friedrich and Wintgen [6] have shown that the bound state in a continuum (BIC) occurs due to the interference of the resonances. If two resonances pass each other as a function of a continuous parameter, then, for a given value of the parameter, one resonance has an exactly vanishing width. Later, this result was reproduced when applied to different physical systems in the two-level approximation [7–12]. A straight waveguide with an attractive, finite-sized impurity presents an example of the realistic structure in which Kim et al. presented numerical evidence for the BIC for a variation in the impurity size [13]. Furthermore, calculations in microwave and semiconductor open structures showed that the resonance width can also turn to zero for a variation in the angle of the bent waveguide [14], the shape of the quantum dot (or resonator) [12, 15], or the magnetic field [16]. Recently, it was rigorously shown that the zero resonance width is the necessary and sufficient condition for BIC [16, 17]. This condition means that the coupling of the resonance state with a continuum equals zero to convert the state into BIC [18, 16].

That very restricted list of references shows that BICs might occur in different open quantum systems including, for example, laser-induced continuum structures in atoms [19], in the molecular system [20]. However, when applied to open quantum dots (QD), BICs were studied in the single electron approximation, whereas the Coulomb interactions between electrons might be very important for the robustness of the BIC. In the present work, we consider the effect of local intradot Coulomb interactions in QDs onto BICs within the framework of the two-level impurity Anderson model [21], which is one of the most important theoretical models for the study of strong correlations in condensed matter physics.

We consider QDs coupled to leads (left and right) which support one propagating mode (the case of two continuums) with the following total Hamiltonian:

$$H = \sum_{C=L,R} H_C + H_D + V. \quad (1)$$

The leads, left L and right R , in (1) are presented as the noninteracting electron gas

$$H_C = \sum_{k\sigma} \epsilon(k) c_{k\sigma C}^+ c_{k\sigma C}, \quad C = L, R. \quad (2)$$

A continual spectrum $\epsilon(k)$ defines the propagating band of leads. The Hamiltonian of a many-level QD is that of the impurity Anderson model [21],

$$H_D = \sum_{m\sigma} \epsilon_m a_{m\sigma}^+ a_{m\sigma} + \sum_m U_m n_{m\sigma} n_{m\bar{\sigma}}. \quad (3)$$

[¶]The text was submitted by the authors in English.

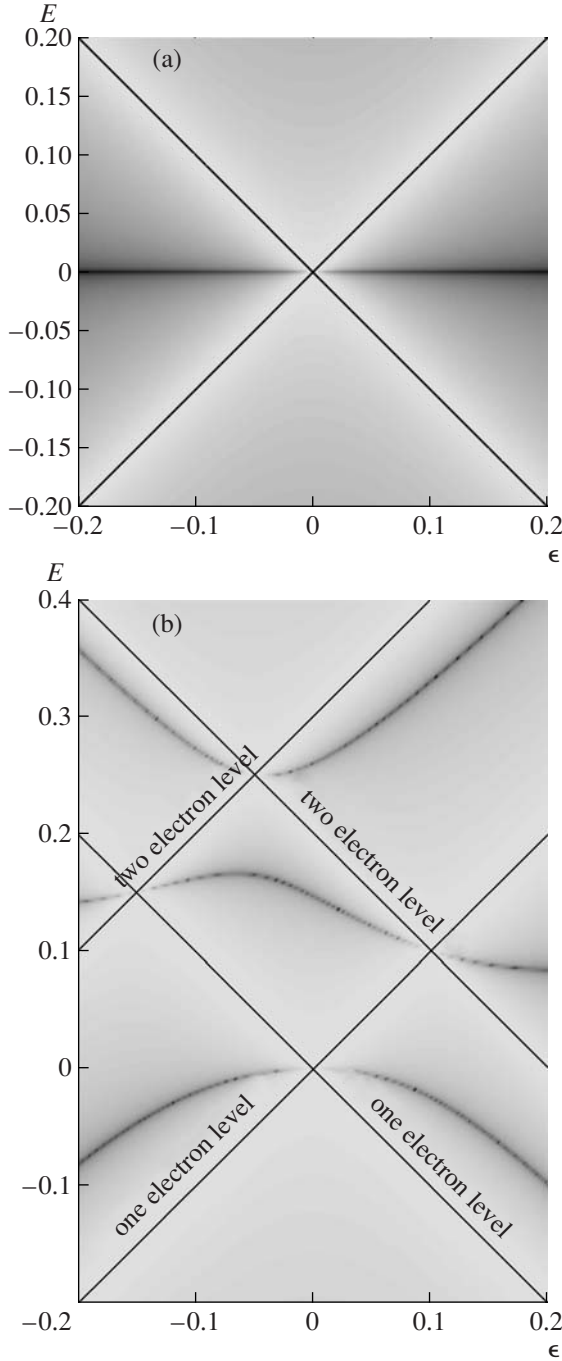


Fig. 1. (a) The transmission $\ln|T|$ of the QD versus the energy of the incident electron and energy splitting ϵ for the case of zero Hubbard repulsion $U_1 = U_2 = 0$. (b) The case of a strong Hubbard repulsion $U_1 = 0.2$, $U_2 = 0.3$, and $\Gamma_1 = \Gamma_2 = 0.05$. The single-electron and two-electron energy levels in closed QDs are shown by the thin lines. The black regions correspond to those where the transmission is close to zero, while the white regions correspond to the maximal transmission.

Here, $a_{m\sigma}^+$ is the creation operator of an electron on the m th level of the QD, U_m takes into account the Hubbard

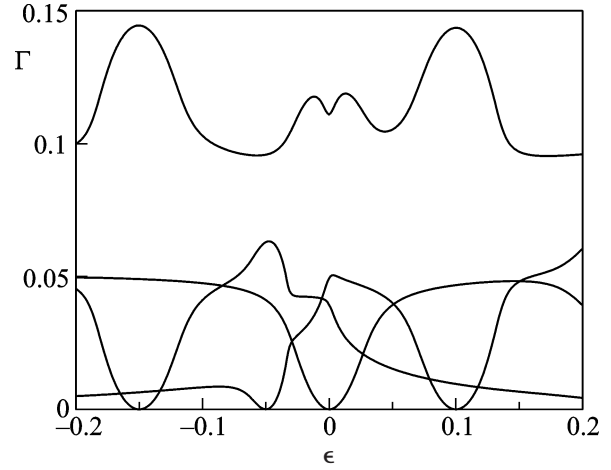


Fig. 2. Resonance widths deemed as $-2\text{Im}[z_\lambda(E, \epsilon)]$, $\lambda = 1, 2, 3, 4$ versus ϵ for $E = 0$, where z_λ are the poles of Green's function (5).

repulsion at the level m , and $n_{m\sigma} = a_{m\sigma}^+ a_{m\sigma}$. The interaction

$$V = \sum_{k\sigma m C} V_m(k) (c_{k\sigma C}^+ a_{m\sigma} + \text{h.c.}) \quad (4)$$

describes the couplings between the leads and QD, where $c_{k\sigma C}^+$ is the creation operator of an electron in the lead C .

In order to calculate the transport properties of the QD, we use a technique of the equations of motion for retarded and advanced Green's functions, which were successfully used to consider the Fano and Kondo resonances in the Anderson model [22–27]. Following Lacroix [28], we use a Hartree–Fock approximation in the wires $\langle\langle c_{k\sigma C} a_{n\bar{\sigma}}^+ a_{n\bar{\sigma}} | a_{m\sigma}^+ \rangle\rangle \approx \langle n_{n\bar{\sigma}} \rangle \langle\langle c_{k\sigma C} | a_{m\sigma}^+ \rangle\rangle$. The approximation is justified for weak couplings compared to the Coulomb interactions: $V_m \ll U_m$. As a result, we obtain the following equation:

$$\mathbf{G}^{-1}(E) = \mathbf{G}_{QD}^{-1}(E) + i\Gamma \quad (5)$$

for the Green's functions $G_{m\sigma, n\sigma}(E) = \langle\langle a_{m\sigma} | a_{n\sigma}^+ \rangle\rangle^{-1}$ in the form of the Dyson equation [24]. Here, $\mathbf{G}_{QD}(E)$ is the Green's function of the isolated QD

$$G_{QD, mm', \sigma, \sigma'}(E) = G_{QD, m\sigma}(E) \delta_{mm'} \delta_{\sigma, \sigma'},$$

$$G_{QD, m\sigma}(E) = \frac{1 - \langle n_{m\bar{\sigma}} \rangle}{E - \epsilon_m} + \frac{\langle n_{m\bar{\sigma}} \rangle}{E - \epsilon_m - U_m}, \quad (6)$$

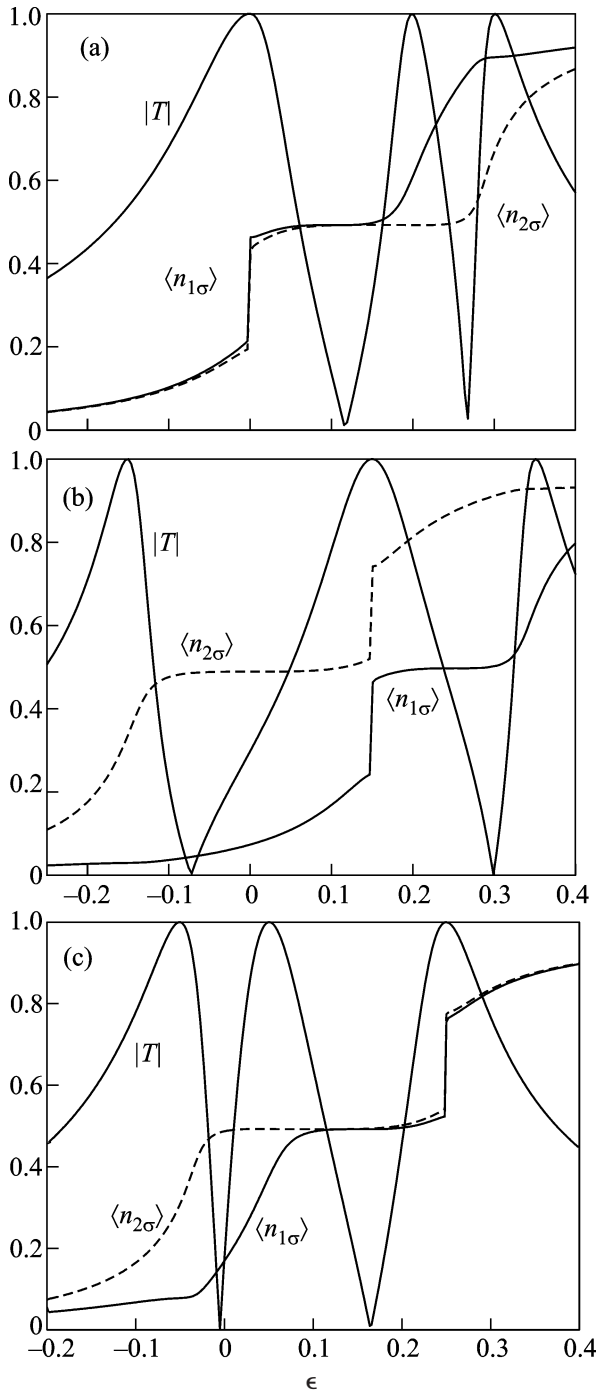


Fig. 3. Electron populations dependent on the energy of the incident electron defined by (8) for the parameters of the system given in Fig. 1: (a) $\epsilon = 0$, (b) $\epsilon = -0.15$, and (c) $\epsilon = -0.05$.

which are exact for the isolated QD. For simplicity, we take wide band wires and approximate the self-energy as [29, 24]

$$\sum_k \frac{V_m(k)V_n(k)}{E - \epsilon(k)_\sigma + i0} = -i\pi V_m V_n \rho_C(E) = (-i\sqrt{\Gamma_m \Gamma_n}), \quad (7)$$

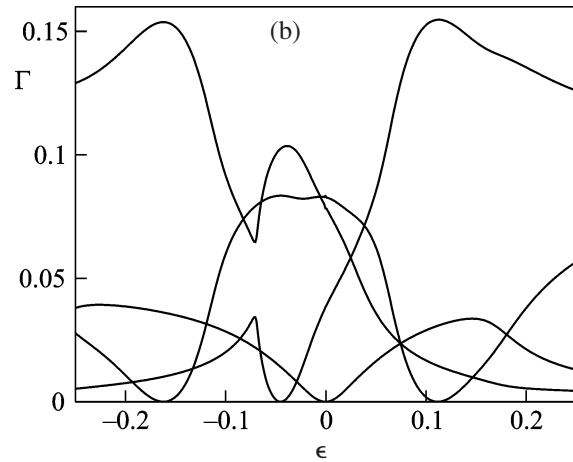
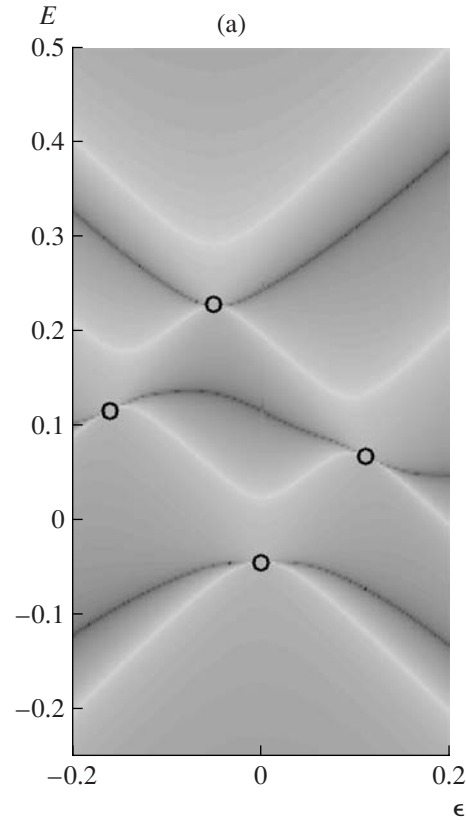


Fig. 4. (a) The transmission $\ln(-\ln(1-|T|))$ of the QD versus the energy of the incident electron and energy splitting ϵ in the avoiding crossing scenario $v=0.05$, $U_1=0.2$, $U_2=0.3$, and $\Gamma_1=\Gamma_2=0.05$. The black regions correspond to those where the transmission is close to zero, while the white regions correspond to those where the transmission is near unity. Therefore, the white regions follow the single-electron and two-electron energy levels in closed QDs. The positions of the BICs are shown by open circles. (b) The resonance widths as shown in Fig. 2b, but in the avoiding crossing scenario.

where $\rho_C(E)$ is the density of states for the left and right wires. The average values of the occupation numbers $\langle n_{m\sigma} \rangle = \langle a_{m\sigma}^+ a_{m\sigma} \rangle$ which enter the expressions for the

Green's functions are calculated self-consistently via the formulas [28]

$$\langle n_{m\sigma} \rangle = \frac{1}{\pi} \int dE \text{Im} G_{m\sigma, m\sigma}(E). \quad (8)$$

The form of self-energy (7) and QD Green's function (6) allow us to proceed to the case of the free electrons with $U_m = 0$. In this case, BIC appears if the QD acquires accidental degeneracy $\epsilon_1 = \epsilon_2$ [12]. Therefore, in the vicinity of the degeneracy point $\epsilon = \epsilon_2 - \epsilon_1 = 0$, we can restrict ourselves to the two-level approximation for a QD [9]. Then, occupation numbers (8) are given by the four poles of Green's function (5). At zero temperature, the transmission amplitude can be expressed in terms of the Green's function

$$T = \Gamma G(E) \Gamma^+, \quad \Gamma = (\Gamma_1, \Gamma_2). \quad (9)$$

The results of the numerical self-consistent calculation of transmission (9) are presented in Fig. 1. Figure 1a shows the case of zero Hubbard repulsion $U_m = 0$ (no electron correlations) in which the QD is given only by the single-electron energy levels. As shown in [9, 12], BIC occurs here at the point of degeneracy of the electron states in QD for $\epsilon = 0$. At this point, the S matrix becomes singular because the transmission zero crosses the unit transmission [12] as shown in Fig. 1, where the unit transmission follows the energy levels. As the Hubbard repulsion is included, the QD is given not only by single-electron states, but also by the two-electron states as shown in Fig. 1b by solid lines. As a result, we find that the number of degenerated points becomes four as seen from Fig. 1b. One can see that the lines of zero transmission cross the lines of the maximal unit transmission at these points. Therefore, one can expect the BICs at four points of degeneracy of the QD. In order to show this, in Fig. 2, we present the resonance widths of the energy levels defined as $\Gamma_\lambda = -2\text{Im}(z_\lambda)$, $\lambda = 1, 2, 3, 4$, where $z_\lambda(E, \epsilon)$ are the poles of the Green's function or the zeroes of the right-hand expression in Dyson equation (5). The points at which $\Gamma_\lambda = 0$ define the BICs [16, 17]. One can see that these points coincide with the points of degeneracy of the QD given by the equations $\epsilon_{c1} = 0$, $\epsilon_{c2} = U_1/2$, $\epsilon_{c3} = -U_2/2$, and $\epsilon_{c4} = (U_2 - U_1)/2$. The corresponding energies of the BICs are 0, 0.1, -0.15, and 0.05. The first BIC is a pure single-electron localized state superposed of two single-electron states with $m = 1, 2$ [12]. However, the next two BICs are superpositions of the single-electron states and two-electron states. Finally, for the last case ($\epsilon_{c4} = (U_2 - U_1)/20$), the BIC is superposed of the two-electron states in the QD. Although the specific values of Γ_m have no importance for the BIC points defined by the crossings of the

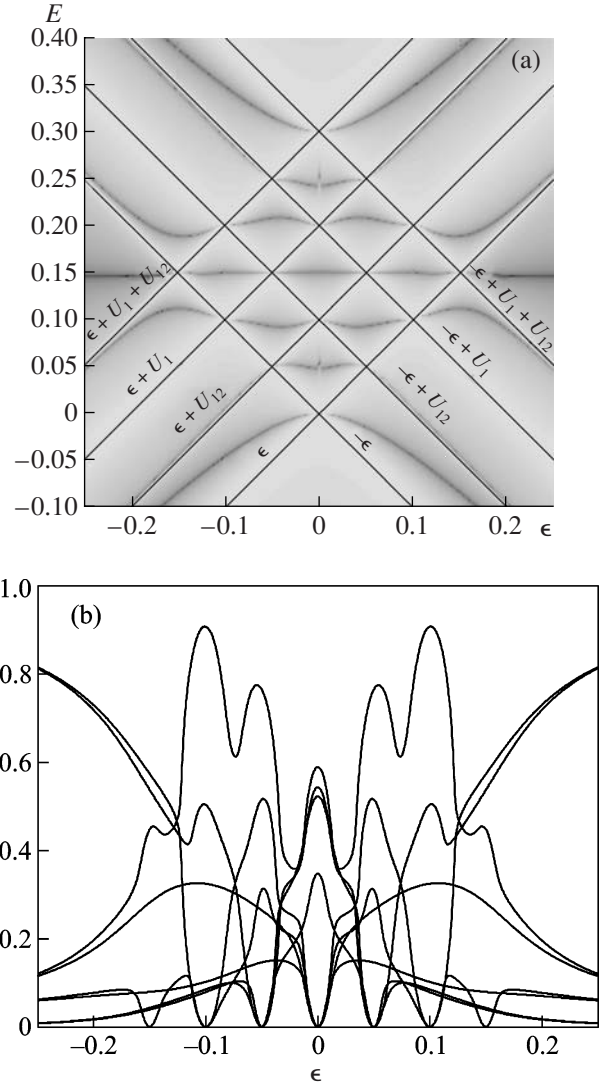


Fig. 5. Same as in Fig. 4 but with inclusion of the interlevel Coulomb interactions $U_{12} = 0.1$. (a) The transmission $\ln|T|$ of the QD versus the energy of the incident electron and energy splitting ϵ in the avoiding crossing scenario $v = 0.05$, $U_1 = U_2 = 0.2$, and $\Gamma_1 = \Gamma_2 = 0.1$. (b) The resonance widths defined as $-2\text{Im}[z_\lambda(E, \epsilon)]$, $\lambda = 1, 2, \dots, 8$ versus ϵ for $E = 0$, where z_λ are the poles of Green's function (10).

energy levels of the QD, they are important for the appearance of the Dicke superradiant state which accumulates the total width [9], as seen from Fig. 2.

Since the resonance width turns to zero when approaching the BIC point, we expect a singular behavior of occupation numbers (8) at the energy of the BIC. In fact, Figs. 3a, 3b, and 3c demonstrate this effect. Let us consider the first BIC at $\epsilon = 0$ with the discrete energy $E = 0$ at which the single-electron energies in the QD are crossing as shown in Fig. 1b. One can see from Fig. 3a that, at the energy $E = 0$, both energy levels are sharply and simultaneously populated up to one-half. The next resonances with finite widths correspond to

the two-electron energies of the QD that are populated smoothly at the Hubbard repulsive energies $U_1 = 0.2$ and $U_2 = 0.3$ by the usual scenario as seen from Fig. 3a.

The next BICs happen when the single-electron state crosses the two-electron state at the points $\epsilon = -0.15$ and $\epsilon = 0.1$. Because of the similarity of these BIC points, we have presented here only the first case as shown in Fig. 3b. The BIC discrete energy for that case is $E = 0.15$ (Fig. 1). Again, we see that, when approaching this energy, the BIC populates sharply. However, the populations of the single-electron and two-electron levels are well separated because of the Hubbard repulsion of the two-electron state. The last figure in Fig. 3c refers to the crossing of two-electron energies at the point $\epsilon = -0.05$. As seen from Fig. 1a, the two-electron BIC has the energy $E = 0.25$. As a result, when approaching this energy, we observe a sharp population of this state similar to the case in (a).

Are BICs critical for the energy-level crossing? Similar to [9, 12], we lift the degeneracy in the QD by the transitions between levels, adding a hopping term between the single-electron states into the Hamiltonian of the two-level QD, $H_D \rightarrow H_D - va_{1\sigma}^+ a_{2\sigma} - va_{2\sigma}^+ a_{1\sigma}$

which evolves from the picture of the energy crossing into the picture with an avoided crossing. Figure 4a shows the transmission of the QD in which the energy levels repel each other, because of the hopping between the QD levels. In order to show clearly the zero and unit transmission, we present the transmission in the double log scale $\ln(-\ln(1 - |T|))$. One can see the avoided level crossings shown by the white lines with $T = 1$. The BICs shown by the open circles are located at those points, where the unit transmission $T = 1$ (white lines) crosses zero at $G = 0$ (black lines) similar to the case of the noninteracting electrons [12]. Figure 4b shows that the resonance widths turn to zero at four critical values of ϵ .

The Hubbard repulsion presented in Anderson impurity model (3) is not the only way to account for the Coulomb interactions. The last interaction also induces the interlevel couplings in the form $\sum_{mn} \sum_{\sigma\sigma'} U_{mn} n_{m\sigma} n_{n\sigma'}$. Therefore, in the two-level approach, a new Coulomb constant U_{12} appears. The equations of motion for the Green's functions in the QD become tedious, but are still complete to give the following Green's function:

$$G_{QD, m\sigma}(E) = \frac{(E + E_m)(E + E_m - U_m - U_{12}\langle n_{\bar{m}\sigma} \rangle)(E + E_m - U_{12} - U_m\langle n_m \rangle)}{(E + E_m - U_m(1 - \langle n_{m\sigma} \rangle) - U_{12}\langle n_{\bar{m}\sigma} \rangle)(E + E_m - U_{12}(1 - \langle n_{\bar{m}\sigma} \rangle) - U_m\langle n_{\bar{m}\sigma} \rangle)(E + E_m - U_m - U_{12}\langle n_{\bar{m}\sigma} \rangle)}, \quad (10)$$

where $m = 1, 2$, $\bar{m} = 2, 1$, and $E_m = \mp\epsilon$. The substitution of (10) into Eqs. (5), (8), and (9) allows for the calculation of the transmission of the QD presented in Fig. 5a. Each crossing of the energy levels shown by the solid lines yields an increase in the BICs as shown in Fig. 5b. One can see that, for $\epsilon = 0$, there are simultaneously four crossings. As a result, at this point, four resonance widths turn to zero as shown in Fig. 5b. Corresponding to the points $\epsilon = \pm 0.05$, we obtain three BICs and so on. If we compare all of the figures with the transmission probability through the QD, one can see that the Coulomb interactions in the QD replicate the transmission zeroes, which are between neighboring resonances. If the resonances are crossing due to the effect of a gate voltage, we observe BICs at each crossing point [6] as shown in Figs. 2, 4b, and 5b.

A.F.S. is grateful to Igor Sandalov for helpful discussions.

REFERENCES

1. J. von Neumann and E. Wigner, Phys. Z. **30**, 465 (1929).
2. F. H. Stillinger and D. R. Herrick, Phys. Rev. A **11**, 446 (1975).
3. D. R. Herrick, Physica B **85**, 44, 270 (1977).
4. F. H. Stillinger, Physica B **85**, 270 (1977).
5. F. Capasso et al., Nature (London) **358**, 565 (1992).
6. H. Friedrich and D. Wintgen, Phys. Rev. A **32**, 3231 (1985).
7. T. V. Shahbazyan and M. E. Raikh, Phys. Rev. B **49**, 17123 (1994).
8. S. Fan, P. R. Villeneuve, J. D. Joannopoulos, and H. A. Haus, Phys. Rev. Lett. **80**, 960 (1998).
9. A. Volya and V. Zelevinsky, Phys. Rev. C **67**, 054322 (2003).
10. M. L. Ladrón de Guevara, F. Claro, and P. A. Orellana, Phys. Rev. B **67**, 195335 (2003).
11. I. Rotter and A. F. Sadreev, Phys. Rev. E **69**, 066201 (2004); Phys. Rev. E **71**, 046204 (2005).
12. A. F. Sadreev, E. N. Bulgakov, and I. Rotter, Phys. Rev. B **73**, 235342 (2006).
13. C. S. Kim, A. M. Satanin, Y. S. Joe, and R. M. Cosby, Phys. Rev. B **60**, 10962 (1999).
14. O. Olendski and L. Mikhailovska, Phys. Rev. B **66**, 035331 (2002).
15. G. Ordóñez, K. Na, and S. Kim, Phys. Rev. A **73**, 022113 (2006).
16. E. N. Bulgakov, K. N. Pichugin, A. F. Sadreev, and I. Rotter, JETP Lett. **84**, 508 (2006).
17. E. N. Bulgakov, I. Rotter, and A. F. Sadreev, Phys. Rev. A **75**, 067401 (2007).

18. C. Texier, J. Phys. A: Math. Gen. **35**, 3389 (2002).
19. A. I. Magunov, I. Rotter, and S. I. Strakhova, J. Phys. B: At. Mol. Opt. Phys. **32**, 1669 (1999).
20. L. S. Cederbaum, R. S. Friedman, V. M. Ryaboy, and N. Moiseyev, Phys. Rev. Lett. **90**, 13001 (2003).
21. P. W. Anderson, Phys. Rev. **124**, 41 (1961).
22. Y. Meir and N. S. Wingreen, Phys. Rev. Lett. **68**, 2512 (1992).
23. H. Haug and A.-P. Jauho, *Quantum Kinetics in Transport and Optics of Semiconductors* (Springer, Berlin, 1996).
24. H. Lu, R. Lü, and B.-F. Zhu, Phys. Rev. B **71**, 235320 (2005).
25. W. Rudziński, J. Barnaś, R. Śewirkowicz, and M. Wilczyński, Phys. Rev. B **71**, 205307 (2005).
26. V. Meden and F. Marquardt, Phys. Rev. Lett. **96**, 146801 (2006).
27. P. Trocha and J. Barnaś, arXiv:0711.3611v1 (2007).
28. C. Lacroix, J. Phys. F: Metal Phys. **11**, 2389 (1981).
29. A. C. Hewson, Phys. Rev. **144**, 420 (1966).